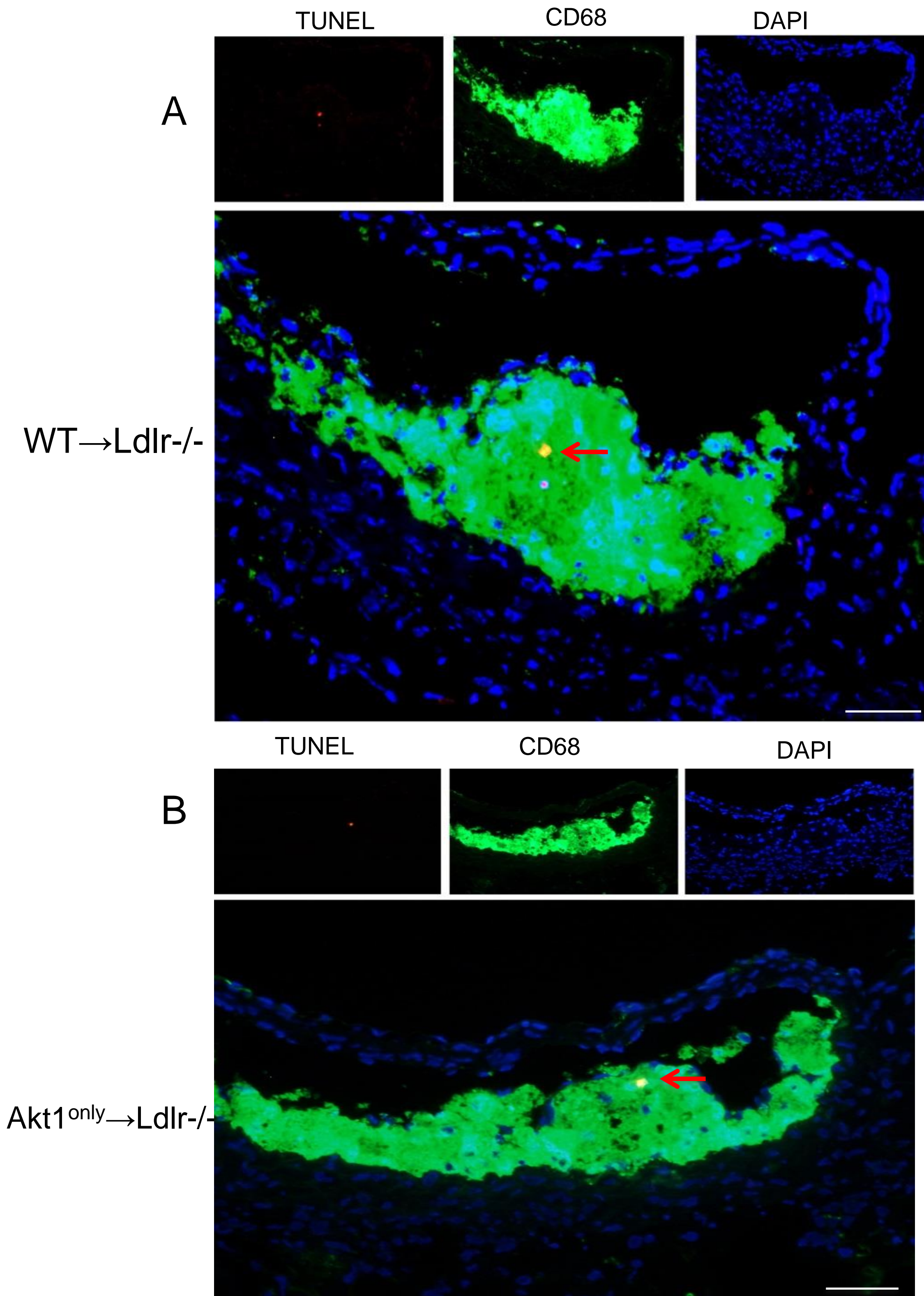

Figure I. **Identification of apoptotic macrophages in atherosclerotic lesions of *Ldlr$^{-/-}$* mice reconstituted with WT (A) or Akt1^{only} FLC (B).**
Double staining for TUNEL (red color) and macrophage marker CD68 (green color) together with DAPI (blue). The set of images with detection of apoptotic cells, macrophages and nuclei separately (top row) and the merge of these images (bottom row); Scale bar is 50μm.

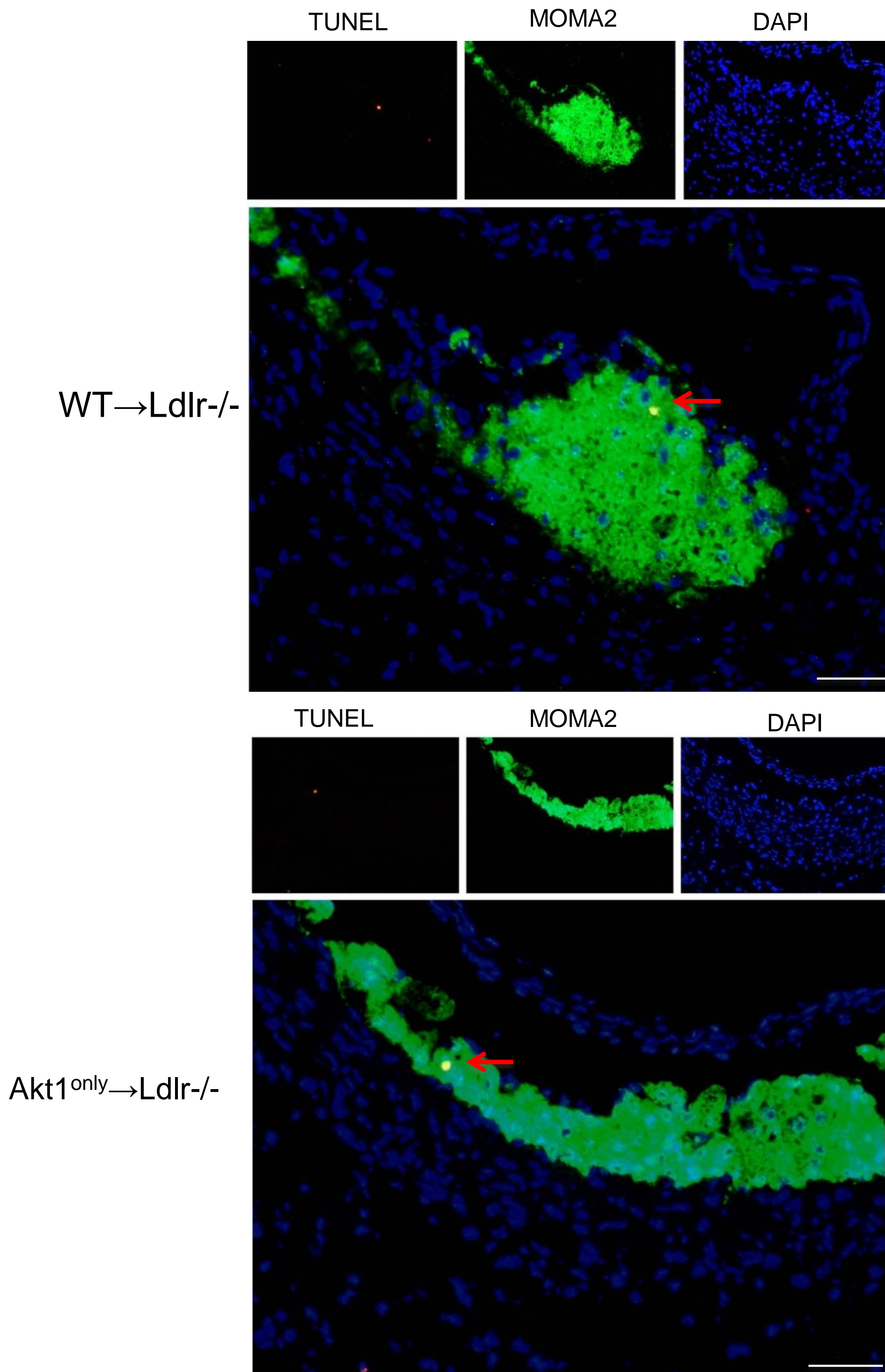

Figure II. **Identification of apoptotic macrophages in atherosclerotic lesions of *Ldlr$^{-/-}$* mice reconstituted with WT (A) or Akt1^{only} FLC (B).**
Staining TUNEL (red color) and macrophage marker MOMA2 (Serotec, cat# MCA519G) (green color) together with DAPI (blue). The set of images with detection of apoptotic cells, macrophages and nuclei separately (top row) and the merge of these images (bottom row); Scale bar is 50μm.

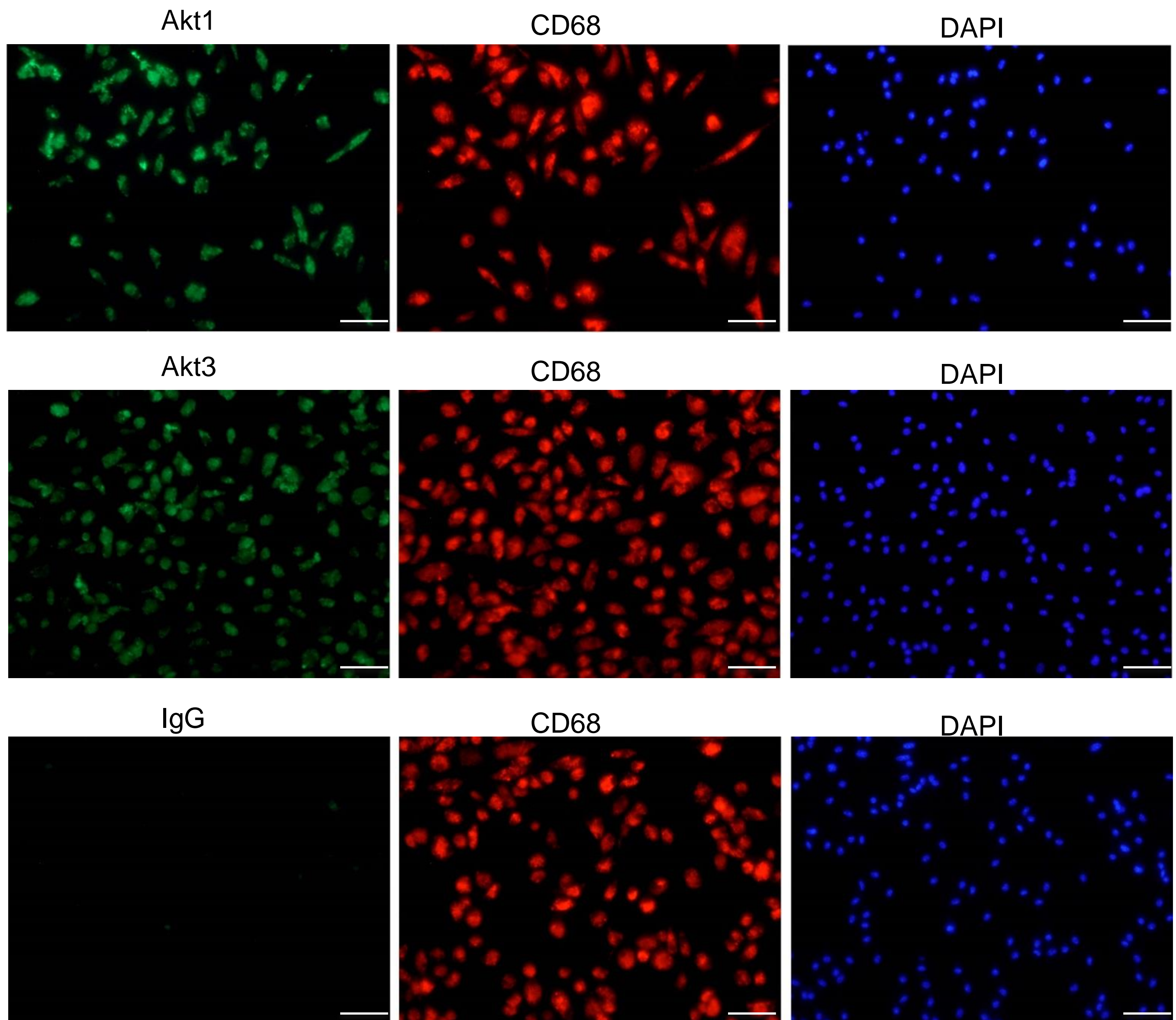

Figure III. **Detection of Akt1 or Akt3 isoforms in cultured macrophages.**
Peritoneal macrophages were collected and two days later stained for Akt1, Akt3 or isotype control IgG (green color) combining with macrophage marker CD68 (red color) and DAPI (blue color). Note specific staining of Akt1 and Akt3 but not isotype control co-localized with macrophages and nucleus stain; Scale bar is 50μm.

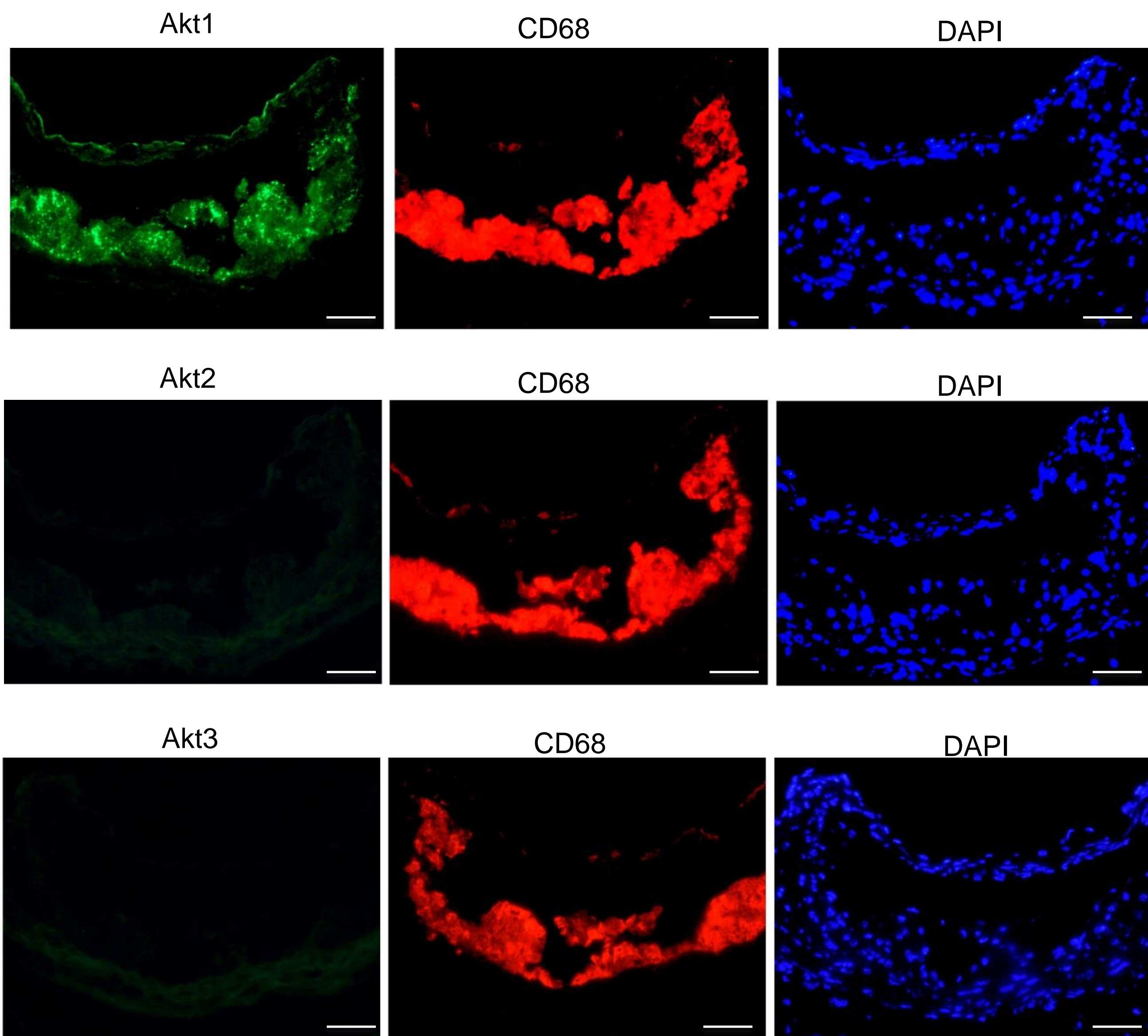

Figure IV. **Detection of Akt1, Akt2 and Akt3 isoforms in atherosclerotic lesions of mice reconstituted with Akt1^{only} FLC.**

Serial aortic cross-sections were stained with antibodies to Akt1, Akt2 or Akt3 (green color) combining with macrophage marker CD68 (red color) and DAPI (blue color). Note specific staining of Akt1 but not Akt2 and Akt3 isoforms in macrophage-rich atherosclerotic lesions; Scale bar is 50μm.

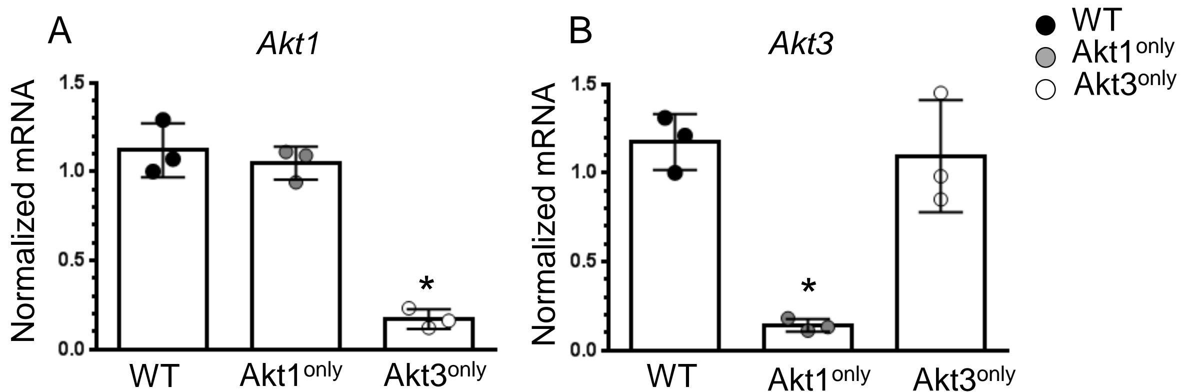

Figure V. ***Akt1* and *Akt3* gene expression levels in WT, Akt1^{only} and Akt3^{only} macrophages.** (**A-B**) Peritoneal macrophages were isolated from mice reconstituted with WT, Akt1^{only} or Akt3^{only} FLC, total RNA was extracted and the gene expression was measured by real-time PCR. Graphs represent data (mean ± SEM) obtained from the same number of mice (n=3/group); *p<0.001 by One Way Analysis of Variance, multiple comparison procedures (Tukey Test).

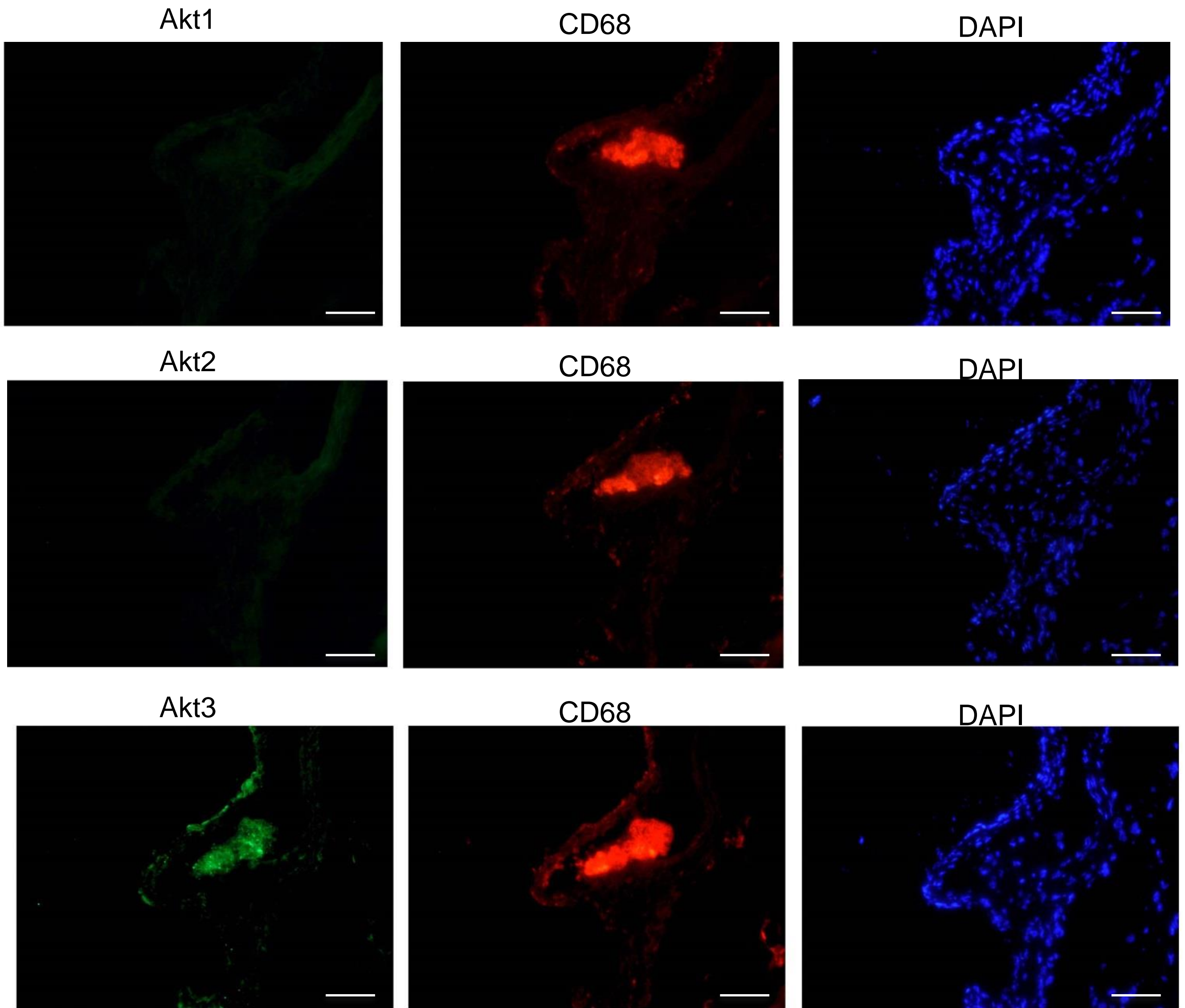

Figure VI. **Detection of Akt1, Akt2 and Akt3 isoforms in atherosclerotic lesions of mice reconstituted with Akt3^{only} FLC.**
Serial aortic cross-sections were stained for Akt1, Akt2 or Akt3 (green color) combining with macrophage marker CD68 (red color) and DAPI (blue color). Note specific staining of Akt3 but not Akt1 and Akt2 isoforms in macrophage-rich atherosclerotic lesions; Scale bar is 50μm.

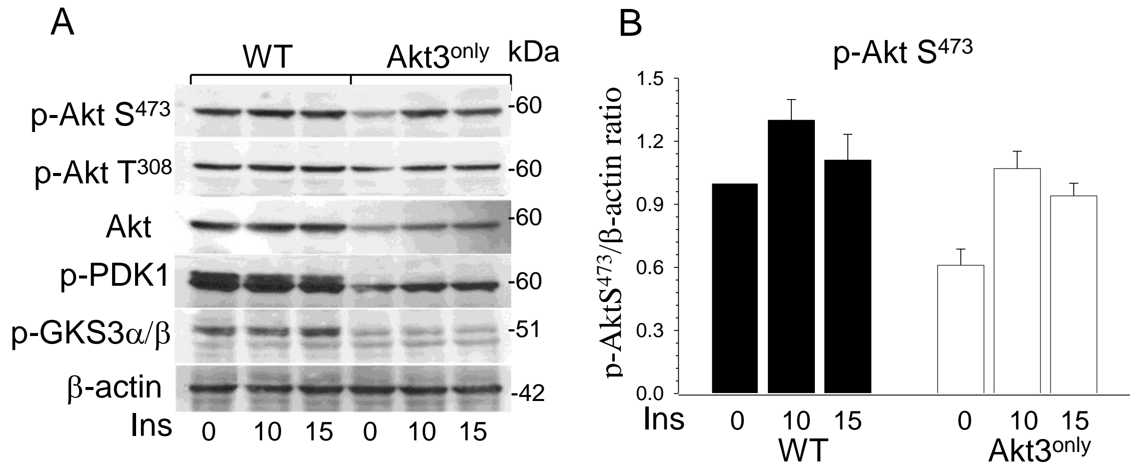

Figure VII. **Akt signaling in WT(■) and Akt3^{only}(□) macrophages**. Peritoneal macrophages were incubated with serum-free media overnight and then untreated or treated with insulin (100nM) for 10 and 15min. Proteins were extracted, resolved and analyzed by Western blot.

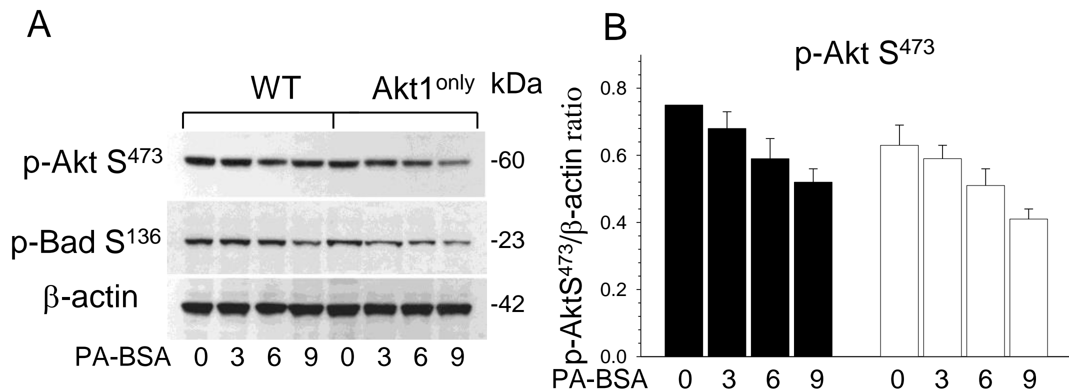

Figure VIII. **ER stress inhibits Akt signaling faster in macrophages expressing only Akt1^{only} compared to WT cells**. WT (■) and Akt1^{only}(□) peritoneal macrophages were treated with BSA or 0.5M PA-BSA for 0, 3, 6 and 9 hours. Extracted proteins were used for analysis of p-Akt and p-Bad signaling. Graphs represent data (mean ± SEM) of three experiments; Note Akt1^{only} cells exhibited higher loss of Akt and Bad phosphorylation during PA-BSA treatment.

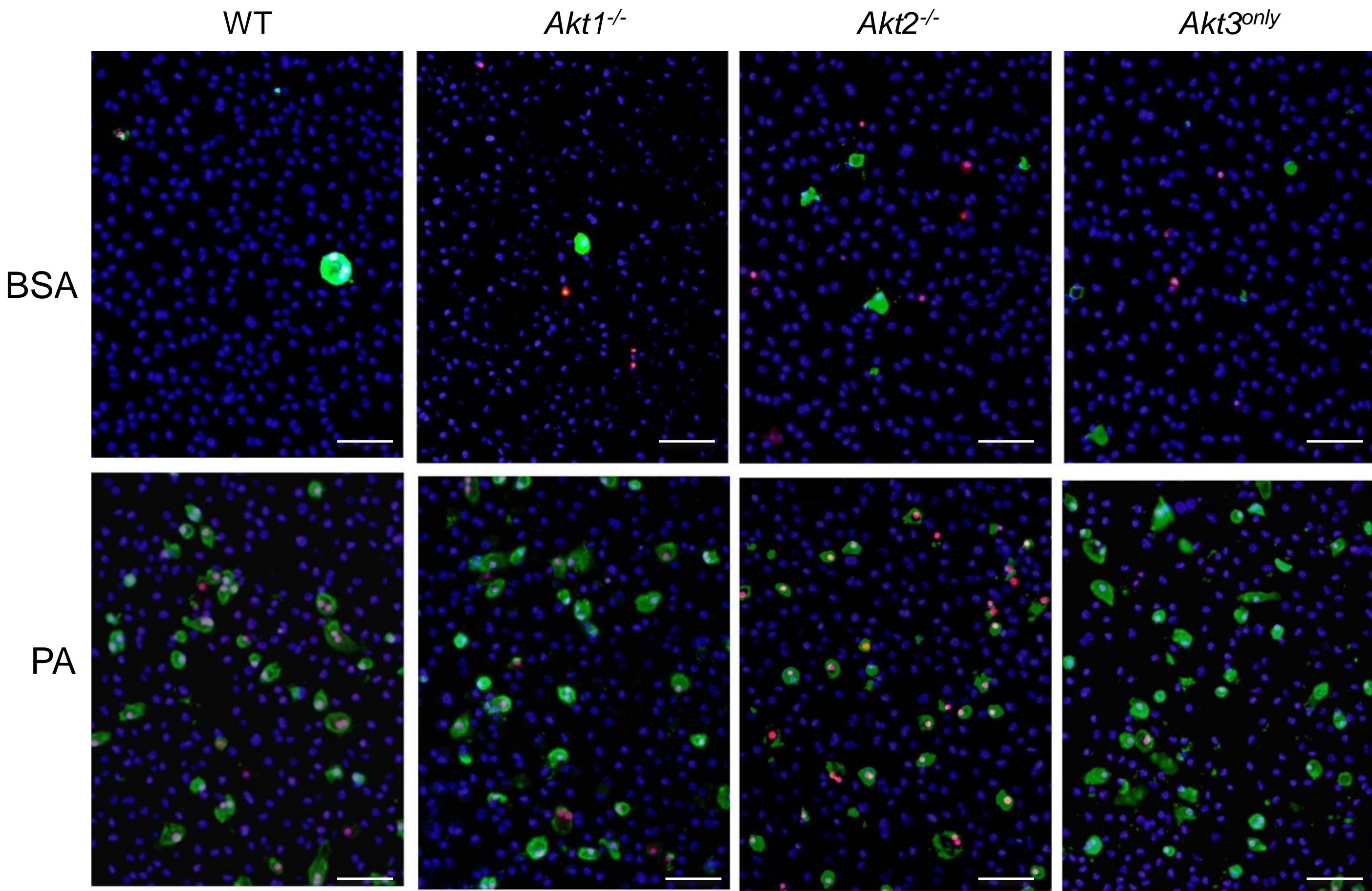

Figure IX. **Macrophages with a single Akt3 isoform are more sensitive to pro-apoptotic stimuli compared to Akt1$^{-/-}$, Akt2$^{-/-}$ and WT cells**

Detection of apoptotic cells in WT, *Akt1$^{-/-}$*, *Akt2$^{-/-}$* or *Akt3^{only}* peritoneal macrophages after treatment with BSA or 0.5mM PA-BSA overnight; Scale bar is 50mm.

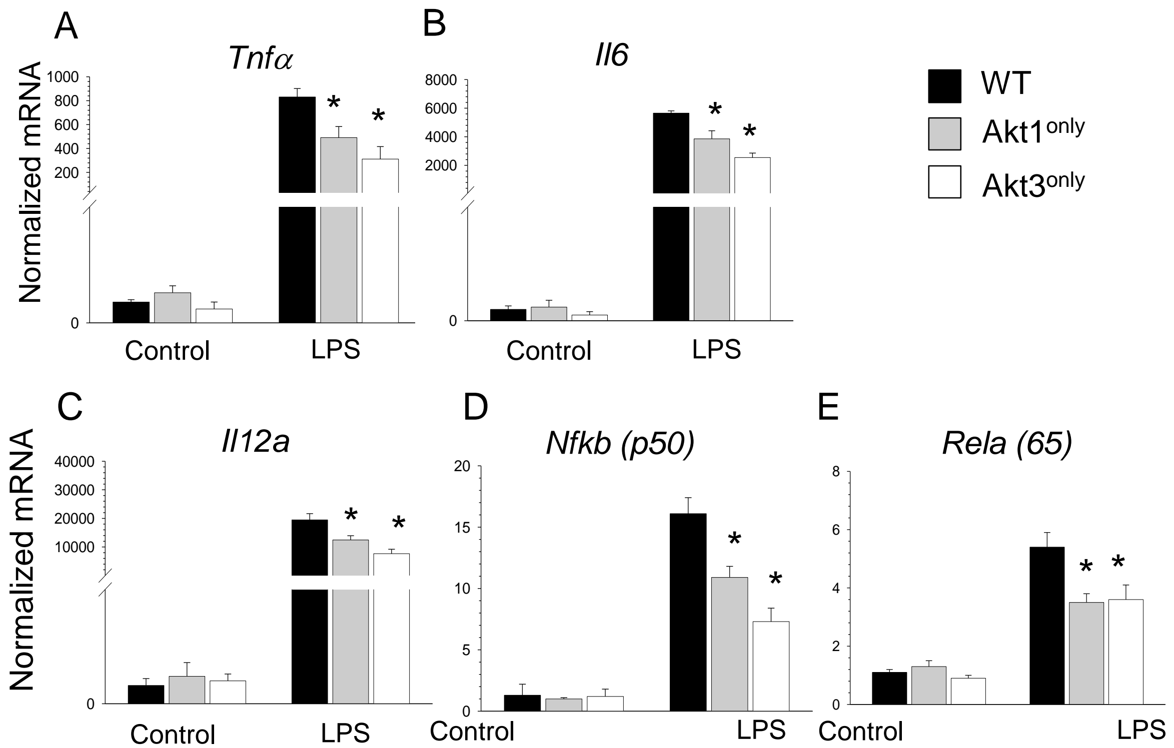

Figure X. **Macrophages with a single Akt isoform express lower levels of inflammatory genes compared to WT cells (A-E)**.

Peritoneal macrophages were isolated from recipient mice reconstituted with WT, Akt1^{only} or Akt3^{only} FLC. Inflammatory gene expression analysis of WT, Akt1^{only} or Akt3^{only} peritoneal macrophages incubated with media alone (control) or LPS (20ng/ml) for 6 hours. Total RNA was isolated and the gene expression assays were measured by real-time PCR. Graphs represent data (mean±SEM) obtained from the same number (n=3/group) of mice (*p<0.05 compared to WT cells treated with LPS by One Way Analysis of Variance).

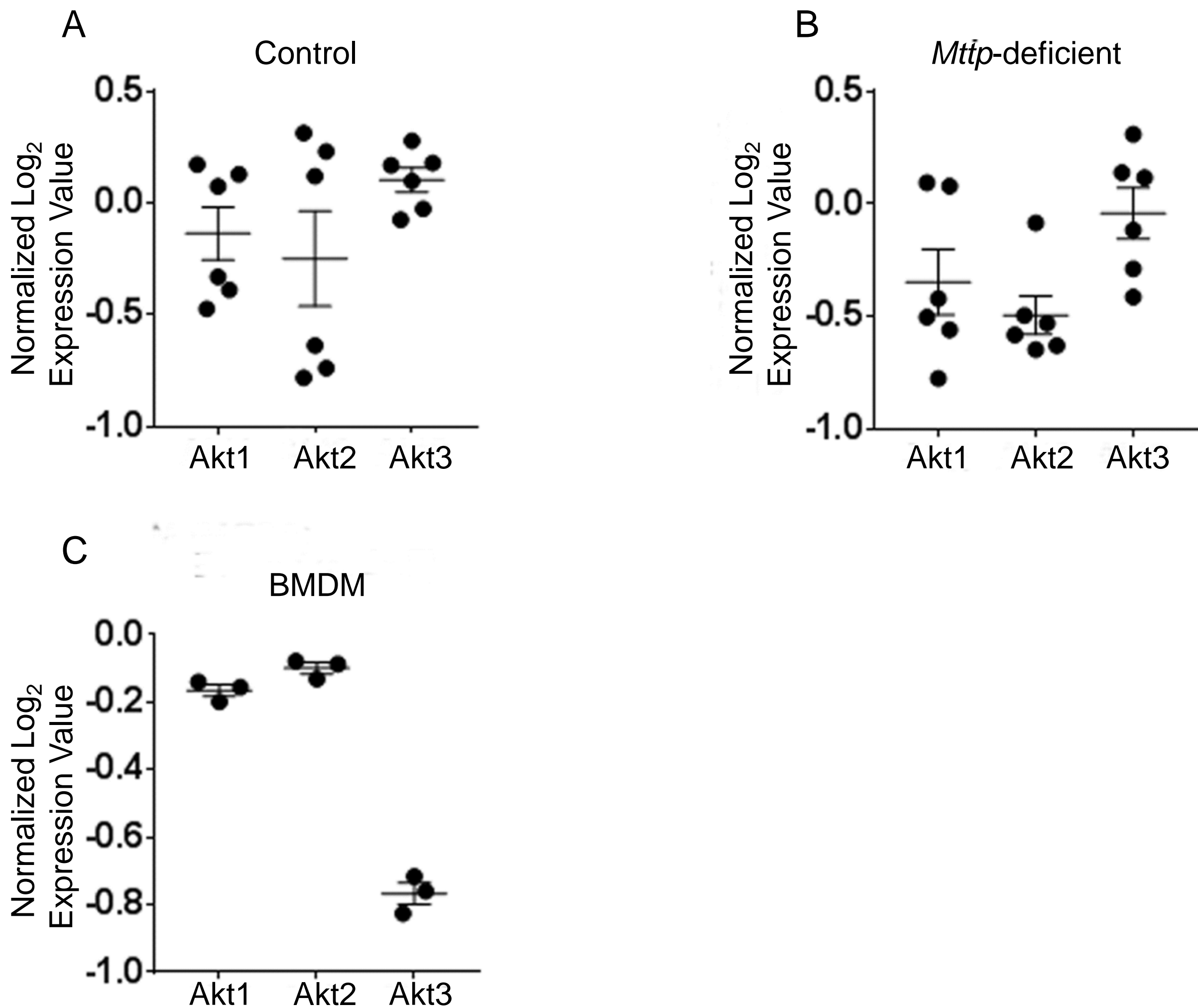

Figure XI: **Meta-analysis of differential Akt1-3 (mRNA) expression across distinct macrophage populations, as quantified by microarrays**.

A,B) $CD68^+$ macrophages isolated by laser capture microdissection from mouse aortic root sections from female *Reversa* mice treated with saline (Control) N=6 (**A**) or polyinosinic: polycytidylic acid (poly I:C) to induce (Mx1)-*Cre* recombinase and delete the floxed microsomal triglyceride transfer protein (*Mttp*) gene in liver. N=6 (**B**).

C) Bone marrow-derived macrophages (BMDM) treated with M-CSF (2500 U/mL) for 7 days. N=3. Meta-analyses were performed on two microarray gene (mRNA) expression datasets publicaly available from NCBI Gene Expression Omnibus (GEO) GSE52482 (Ramsey et al. PloS Genet 2014, 10:e1004828) and ArrayExpress (ww.ebi.ac.uk/arrayexpress) E-MTAB-790 (Lacey et al. J Immunol 2012, 188: 5752). For project GSE52482, Affymetrix.ExonExprChip. MoEx-1_0-st-v1_na32_mm9_2011-06-23 associated .CEL files were analyzed by using GeneSpring GX14.9 (Agilent) and data were summarized by ExonRMA algorithm, quantile normalized, and baseline transformed to the median of all samples. For project E-MTAB-790, Agilent.SingleColor.14868 data were normalized to 75.0^{th} percentile and baseline transformed to the median of all samples. Akt mRNA expression levels were filtered and reported in Log_2.